ORGANOMETALLICS

Article

pubs.acs.org/Organometallics

Steric and Electronic Effects in the Formation and Carbon Disulfide Reactivity of Dinuclear Nickel Complexes Supported by Bis(iminopyridine) Ligands

Amarnath Bheemaraju,[†] Jeffrey W. Beattie,[†] Erwyn G. Tabasan,[†] Philip D. Martin,[†] Richard L. Lord,*[,‡] and Stanislav Groysman*[,†]

[†]Department of Chemistry, Wayne State University, Detroit, Michigan 48202, United States

[‡]Department of Chemistry, Grand Valley State University, Allendale, Michigan 49401, United States

Supporting Information

ABSTRACT: We are developing bimetallic platforms for the cooperative activation of heteroallenes. Toward this goal, we designed a new family of bis(iminopyridine) ((*N*,*N*′-1,1′-(1,4-phenylene)bis(*N*-(pyridin-2-ylmethylene)methanamine) and *N*,*N*′-1,1′-(1,4-phenylene)bis(*N*-(1-(pyridin-2-yl)ethylidene)-methanamine)) dinickel complexes, synthesized their CS_2 compounds, and studied their reactivity. Bis(iminopyridine) ligands L react with $Ni(COD)_2$ to form $Ni_2(L)_2$ complexes or $Ni_2(L)(COD)_2$ complexes as a function of the steric and electronic properties of the ligand precursor. Product structures disclosed an *anti* geometry in the $Ni_2(L)(COD)_2$ species and helical (*anti*) structures for $Ni_2(L)_2$ complexes. Carbon disulfide adducts $Ni_2(L)(CS_2)_2$ were obtained in good yields upon addition of CS_2 to $Ni_2(L)(COD)_2$ or in a one-pot reaction of L with 2 equiv of both $Ni(COD)_2$ and CS_2. $Ni_2(L)(CS_2)_2$ complexes are highly flexible, displaying both *syn* and *anti* conformations (shortest S- - -S separations of 5.0 and 9.5 Å, respectively) in the solid state. DFT calculations demonstrate virtually no energy difference between the two conformations. Electrochemical studies of the $Ni_2(L)(CS_2)_2$ complexes displayed two ligand-based reductions and a broad CS_2-based oxidation. Chemical oxidation with $[FeCp_2]^+$ liberated free CS_2. The addition of NHC (NHC = 1,3-di-*tert*-butylimidazolin-2-ylidene) to $Ni_2(L)(CS_2)_2$ yielded $Ni_2(NHC)_2(CS_2)_2$, in which both carbon disulfide ligands are bridging two Ni centers.

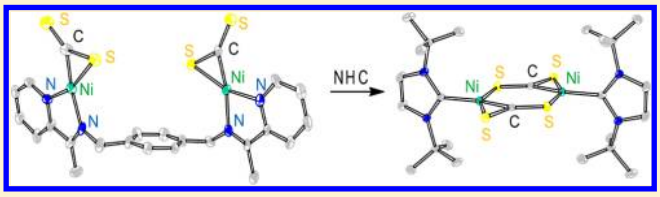

INTRODUCTION

Dinuclear complexes offer an attractive strategy for the cooperative binding and activation of small molecules.[1,2] In particular, heteroallene activation is a multielectron process and the cooperative action of several metals broadens the number of oxidation states available for the heteroallene reduction.[3−6] Recently, several groups reported CO_2 activation and reduction using dinuclear and polynuclear complexes.[7−9] Several different approaches were tested. Thomas and co-workers described a heterodinuclear system containing a metal−metal bond that oxidatively adds CO_2.[7] Berben and co-workers described electrocatalytic reduction of CO_2 to formate by the tetrametallic cluster $[HFe_4N(CO)_{12}]^-$.[8] Hazari and co-workers have investigated insertion of CO_2 into Pd(I) bridging allyl dimers.[9]

We are designing homodinuclear metal complexes for the cooperative activation of heteroallenes (CO_2 and CS_2).[10] Our systems feature metal centers that are positioned close to each other but are connected by a flexible linker and feature no direct metal−metal bond. Our goal is to achieve the reductive transformation of two heteroallene molecules by the cooperative action of two metal centers, brought together by a dinucleating ligand. Possible products of this bimetallic reductive transformation include oxalate (tetrathiooxalate) and carbonate (trithiocarbonate). This goal requires the design of dinuclear systems in which the two heteroallene substrates are close enough to react with each other. Furthermore, the electronic structure of the heteroallene adduct is of primary importance as it determines its reactivity. The electronic structure of a bound heteroallene is determined in part by the ancillary ligand. The current investigation focuses on iminopyridine chelates. Our choice of the iminopyridine ancillary ligand results from its redox-active nature that helps to stabilize low-oxidation-state metal precursors and to mediate electron transfer upon binding and reduction of substrates.[11] Toward this goal, we have recently reported two dinucleating bis(iminopyridine) ligands, L^1 and L^2 (see Figure 1).[10] We discovered that the treatment of the ligand with $Ni(COD)_2$ affords two different products: the expected complex $Ni_2(L^1)(COD)_2$ (**1a**) for L^1 and the bis(homoleptic) complex $Ni_2(L^2)_2$ (**2b**/**2c**) for L^2.[10a] We also reported that $Ni_2(L^1)(COD)_2$ reacts with 2 equiv of carbon disulfide to form $Ni_2(L^1)(CS_2)_2$.[10b] To decipher the steric and electronic effects guiding the formation and the reactivity of the dinuclear nickel complexes, we designed several bis(iminopyridine) ligands featuring different substituents in the ligand's framework. In this work we interrogate the formation, properties, and reactivity of the

Received: March 6, 2013

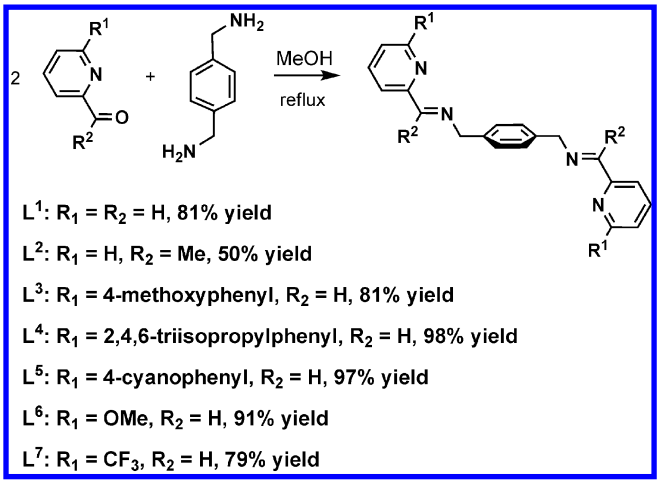

Figure 1. Synthesis of ligands L^1–L^7.

open-chain $Ni_2(L)(COD)_2$-type complexes vs bis(homoleptic) Ni_2L_2-type complexes. In addition, we report the straightforward one-pot synthesis of $Ni_2(L)(CS_2)_2$ complexes that does not require prior isolation of the $Ni_2(L)(COD)_2$ complexes. Electrochemical properties and the reactivity of $Ni_2(L)(CS_2)_2$ complexes are presented. The structure of the *syn*-$Ni_2(L)(CS_2)_2$-type complex is reported and compared with the structure of the *anti*-$Ni_2(L)(CS_2)_2$-type complex. The conformational stability of the arms in this bimetallic complex is interrogated using DFT.

■ EXPERIMENTAL SECTION

General Considerations. All reactions involving metal complexes were executed in a nitrogen-filled glovebox. *p*-Xylylenediamine, 6-(4-methoxyphenyl)-2-pyridinecarboxaldehyde, 6-methoxy-2-pyridinecarboxaldehyde, 4-(6-formylpyridin-2-yl)benzonitrile, 2-bromopyridine-6-carboxaldehyde, 2,4,6-triisopropylphenylboronic acid, 6-(trifluoromethyl)pyridine-2-carboxaldehyde, bis(cyclooctadiene)-nickel(0) ($Ni(COD)_2$), 1,3-di-*tert*-butylimidazolin-2-ylidene (NHC), carbon disulfide, and ^{13}C-labeled carbon disulfide were purchased from Aldrich, Strem, or TCI America and used as received. L^1 and L^2 were synthesized as previously described.[10] All solvents were purchased from Fisher Scientific and were of HPLC grade. The solvents were purified using an MBRAUN solvent purification system and stored over 3 Å molecular sieves. Compounds were routinely characterized by ^1H NMR, $^{13}C\{^1H\}$ NMR (^{13}C NMR thereafter), and ^{19}F NMR spectroscopy, X-ray crystallography, and elemental analyses. Selected compounds were characterized by mass spectrometry (ESI). NMR spectra of all compounds were recorded at the Lumigen Instrument Center (Wayne State University) on a Varian Mercury 400 NMR spectrometer in C_6D_6, $(CD_3)_2SO$ or CD_2Cl_2 at room temperature. Chemical shifts and coupling constants (J) are reported in parts per million (δ) and hertz, respectively. Low-resolution mass spectra were obtained at the Lumigen Instrument Center utilizing a Waters Micromass ZQ mass spectrometer (direct injection, with capillary at 3.573 kV and cone voltage of 20.000 V). Only selected peaks in the mass spectra are reported below. Elemental analyses were performed by Midwest Microlab LLC.

Synthesis and Characterization of Compounds. *L^3*. A 50 mL methanol solution of 6-(4-methoxyphenyl)-2-pyridinecarboxaldehyde (3.61 g, 33.8 mmol) was added to a 50 mL methanol solution of *p*-xylylenediamine (2.3 g, 16.9 mmol). The resulting solution was stirred and refluxed for 4 h. The white cloudy reaction mixture was cooled to room temperature. A white solid was isolated by filtration and dried to give L^3 (4.28 g, 81%). ^1H NMR (CD_2Cl_2, 400 MHz): δ 8.55 (s, 2H), 8.01 (d, J = 8.4, 4H), 7.92 (d, J = 6.4, 2H), 7.77 (t, J = 7.2, 2H), 7.71 (d, J = 7.6, 2H), 7.37 (s, 4H), 6.99 (d, J = 7.2, 4H), 4.87 (d, J = 1.6, 4H), 3.86 (s, 6H). ^{13}C NMR (CD_2Cl_2, 75 MHz): δ 163.89, 161.21, 156.96, 155.03, 138.59, 137.70, 131.96, 128.85, 128.62, 121.03, 119.08, 114.55, 65.16, 55.86. HRMS (ESI): calcd for $[C_{34}H_{30}N_4O_2 + H]^+$ 527.2447, found 527.2438. Mp: 204 °C.

6-(2,4,6-Triisopropylphenyl)-2-pyridinecarboxaldehyde. This compound was prepared in a way similar to that for the previously reported 4-fluoro-2′,4′,6′-triisopropylbiphenyl-3-carbaldehyde.[12] Under a nitrogen atmosphere, 6-bromo-2-pyridinecarboxaldehyde (1.60 g, 8.60 mmol), 2,4,6-triisopropylphenylboronic acid (3.20 g, 12.89 mmol), 2-dicyclohexylphosphino-2′,6′-dimethoxybiphenyl (SPhos; 0.60 g, 1.48 mmol), and K_3PO_4 (20 g, excess base) were added to a 250 mL Schlenk flask. The flask was evacuated and refilled with nitrogen three times. Toluene (35 mL) and $Pd(OAc)_2$ (0.38 g, 1.71 mmol) were added to the flask. The reaction mixture was heated to 110 °C for 48 h. After that, the reaction mixture was cooled to room temperature and diethyl ether (50 mL) was added. The resulting reaction mixture was filtered through a thin pad of silica gel, and the resulting filtrate was concentrated in vacuo. The crude product was purified by silica gel chromatography (5/95 ether/hexanes) to afford the product 6-(2,4,6-triisopropylphenyl)-2-pyridinecarboxaldehyde (0.80 g, 30%) as a white solid. ^1H NMR (C_6D_6, 400 MHz): δ 10.16 (s, 1H), 7.63 (d, J = 7.2, 1H), 7.20 (s, 2H), 6.99 (d, J = 7.2, 1H), 6.96 (q, J = 7.6, 1H), 2.86 (m,, 1H), 2.55 (m, 2H), 1.27 (d, J = 6.8, 6H), 1.12 (t, J = 6.8, 12H). ^{13}C NMR (C_6D_6, 75 MHz): δ 193.57, 161.57, 153.50, 149.98, 147.14, 136.89, 129.36, 128.73, 128.62, 128.14, 121.37, 119.47, 35.29. 31.31, 24.83, 24.71, 24.38; HRMS (ESI): calcd for $[C_{21}H_{27}NO + H]^+$ 310.2171, found 310.2181. Mp: 199 °C.

L^4. A 20 mL methanol solution of 6-(2,4,6-triisopropylphenyl)-2-pyridinecarboxaldehyde (39 mg, 0.12 mmol) was added to a 20 mL methanol solution of *p*-xylylenediamine (85 mg, 0.06 mmol). The resulting solution was stirred and refluxed for 4 h. The reaction mixture was cooled to room temperature. White powder was separated from the solution by filtration, washed with cold methanol, and dried to give L^4 (88 mg, 98%) as a white solid. ^1H NMR (CD_2Cl_2, 400 MHz): δ 8.48 (s, 2H), 8.03 (d, J = 8.0, 2H), 7.78 (t, J = 7.6, 2H), 7.37 (s, 4H), 7.28 (d, J = 7.6, 2H), 7.08 (s, 4H), 4.85 (s, 4H), 2.92 (m, 2H), 2.48 (m, 4H), 1.26 (d, J = 6.8, 12H), 1.07 (dd, J = 3.6, 2.8, 24H). ^{13}C NMR (CD_2Cl_2, 75 MHz): δ 163.99, 160.18, 154.94, 149.69, 146.97, 138.72, 136.79, 136.73, 128.82, 126.69, 121.22, 119.08, 65.22, 35.07, 30.91, 30.27, 24.46, 24.28. HRMS (ESI): calcd for $[C_{50}H_{62}N_4 + H]^+$ 719.5053, found 719.5063. Mp: 255 °C.

L^5. A 20 mL solution of 4-(6-formyl-2-pyridinyl)benzonitrile (200 mg, 0.961 mmol) was added to a 20 mL methanol solution of *p*-xylylenediamine (65.7 mg, 0.481 mmol). The resulting solution was stirred and refluxed for 4 h. The reaction mixture was cooled to room temperature. White precipitate was separated from the solution by filtration, washed with cold methanol, and dried to give L^5 (240 mg, 97%). ^1H NMR (CD_2Cl_2, 400 MHz): δ 8.56 (s, 2H), 8.19 (d, J = 8.4, 4H), 8.06 (dd, J = 6.4, 1.2, 2H), 7.87 (t, J = 7.6, 2H), 7.82 (dd, J = 8.0, 1.6, 2H), 7.77 (d, J = 8.4, 4H), 7.37 (s, 4H), 4.89 (d, J = 1.2, 4H). ^{13}C NMR (CD_2Cl_2, 75 MHz): δ 163.30, 155.58, 155.18, 143.51, 138.52, 138.19, 133.14, 128.93, 127.94, 122.38, 121.02, 119.29, 113.15, 65.16. HRMS (ESI) calcd for $[C_{34}H_{24}N_6 + H]^+$ 517.2141, found 517.2141. Mp: 206 °C.

L^6. A 10 mL methanol solution of 6-methoxy-2-pyridinecarboxaldehyde (250 mg, 1.82 mmol) was added to a 10 mL methanol solution of *p*-xylylenediamine (124 mg, 0.910 mmol). The resulting solution was stirred and refluxed for 4 h. The reaction mixture was cooled to room temperature. White powder was separated from the solution by filtration, washed with cold methanol, and dried to yield L^6 (308 mg, 91%) as a white solid. ^1H NMR (C_6D_6, 400 MHz): δ 8.36 (s, 2H), 7.79 (d, J = 7.6, 2H), 7.25 (s, 4H), 7.01 (t, J = 8.0, 2H), 6.54 (d, J = 8.0, 2H), 4.60 (s, 4H), 3.81 (s, 6H). ^{13}C NMR (C_6D_6, 75 MHz): δ 164.66, 163.0, 153.43, 139.28, 138.76, 128.96, 114.52, 112.69, 64.21, 53.44. HRMS (ESI): calcd for $[C_{22}H_{22}N_4O_2 + H]^+$ 375.1821, found 375.1821. Mp: 121 °C.

L^7. A 50 mL solution of 6-(trifluoromethyl)-2-pyridinecarboxaldehyde (1.00 g, 5.71 mmol) was added to a 50 mL methanol solution of *p*-xylylenediamine (0.389 g, 2.85 mmol). The resulting solution was stirred and refluxed for 4 h. The reaction mixture was cooled to room temperature. White precipitate was separated from the solution by

filtration, washed with cold methanol, and dried to give L^7 (1.01 g, 79%). ^{1}H NMR (C_6D_6, 400 MHz): δ 8.26 (s, 2H), 7.94 (d, J = 8.0, 2H), 7.19 (s, 4H), 6.99 (d, J = 7.6, 2H), 6.82 (t, J = 8.0, 2H), 4.49 (d, J = 1.2, 4H). ^{13}C NMR (C_6D_6, 75 MHz): δ 161.95, 155.96, 148.40, 148.06, 138.42, 137.93, 129.02, 123.67, 121.43, 121.41, 65.02. ^{19}F NMR (C_6D_6, 400 MHz): δ −67.75. HRMS (ESI): calcd for $[C_{22}H_{16}N_4F_6+H]^+$ 451.1357, found 451.1362. Mp: 146 °C.

$Ni_2(L^3)_2$ (3b,c). A suspension of L^3 (62 mg, 0.12 mmol) in 3 mL of THF was added at room temperature to a 3 mL solution of bis(cyclooctadiene)nickel(0) ($Ni(COD)_2$; 65 mg, 0.24 mmol) in THF over the course of 2 h. The reaction mixture was stirred for 24 h to give a purple solution. The solvent was removed under vacuum. The resultant solid was washed with hexane (20 mL) and dissolved in THF (3 mL). The solvent was removed under vacuum to give a dark purple solid. The solid was dissolved in THF (1 mL), ether was added (5 mL), and the resulting mixture was kept at −40 °C for 2 days. The purple crystals that separated were washed with cold ether and dried to afford pure $Ni_2(L^3)_2$ (42 mg, 0.072 mmol, 60%). ^{1}H NMR (C_6D_6, 400 MHz): isomer a, δ 9.12 (s, 4H), 8.63 (d, J = 8.0, 4H), 8.10 (d, J = 6.0, 4H), 7.99 (t, J = 7.2, 4H), 6.94 (s, 8H), 6.68 (d, J = 8.4, 8H), 6.55 (d, J = 10.4, 8H), 5.57 (s, 4H, 1,5-cyclooctadiene), 4.90 (d, J = 13.2, 4H), 3.96 (d, J = 13.4, 4H), 3.22 (s, 12H), 2.20 (s, 8H, 1,5-cyclooctadiene); isomer b, δ 8.86 (s, 4H), 8.51 (d, J = 8.8, 4H), 8.08 (d, J = 6.0, 4H), 7.94 (t, J = 6.8, 4H), 6.92 (s, 8H), 6.64 (d, J = 8.0, 8H), 6.53 (d, J = 8.8, 8H), 4.06 (d, J = 13.6, 4H), 3.72 (d, J = 13.6, 4H), 3.27 (s, 12H). ^{13}C NMR (C_6D_6, 75 MHz): δ 163.87, 163.54, 162.76, 159.58, 159.40, 144.73, 143.86, 138.78, 138.59, 135.44, 134.60, 133.58, 132.81, 129.03, 126.57, 126.12, 122.35, 121.68, 117.65, 116.98, 114.77, 113.0, 68.93, 68.30, 68.15, 66.25, 55.12, 55.07, 15.93. MS (ESI): calcd for $Ni_2(L^3)_2$ ($[C_{68}H_{60}N_8O_4Ni_2]^+$) 1168.34, found 1168.51. Anal. Calcd for $C_{68}H_{60}N_8O_4Ni_2$: C, 69.7; H, 5.1; N, 9.6. Found: C, 69.2; H, 5.5; N, 9.2.

$Ni_2(L^4)_2$ (4b). A suspension of L^4 (70 mg, 0.10 mmol) in 3 mL of THF was added at room temperature to a 3 mL solution of $Ni(COD)_2$ (27 mg, 0.10 mmol) in THF. The reaction mixture was stirred for 24 h to give a purple solution. The solvent was removed under vacuum. The residue was dissolved in hexane (3 mL) and stored at −30 °C to give black crystals in two crops (combined yield 21 mg, 0.027 mmol, 27% yield). ^{1}H NMR (C_6D_6, 400 MHz): δ 9.68 (s, 4H), 8.09 (t, J = 8.0, 4H), 7.92 (d, J = 6.8, 4H), 7.27 (d, J = 1.6, 4H), 7.26 (s, 8H), 6.59 (dd, J = 9.2, 1.2, 4H), 5.12 (d, J = 13.6, 4H), 4.51 (m, 4H), 3.93 (d, J = 13.6, 4H), 2.53 (m, 8H), 1.34 (m, 48H), 1.15 (m, 24H) (note: δ 8.60 (s, 2H), 8.16 (d, J = 7.6, 2H), 7.23 (s, 8H), 7.10 (t, J = 8.0, 2H), 7.00 (d, J = 7.6, 2H), 4.57 (s, 4H), 2.86 (p, J = 7.2, 6.8, 2H), 2.73 (p, J = 6.8, 6.8, 4H), 1.28 (d, J = 6.8, 12H), and 1.17 (dd, J = 11.6, 7.2, 24H) are peaks corresponding to free L^4). MS (ESI): calcd for $Ni_2(L^4)_2$ ($[C_{100}H_{124}N_8Ni_2]^+$) 1552.87, found 1553.07. Anal. Calcd for $C_{100}H_{124}N_4Ni_2$: C, 77.2; H, 8.0; N, 7.2. Found: C, 76.9; H, 8.2; N, 7.0.

$Ni_2(L^4)(COD)_2$ (4a). A suspension of L^4 (33 mg, 0.046 mmol) in 3 mL of THF was added at room temperature to a 3 mL solution of $Ni(COD)_2$ (28 mg, 0.10 mmol) in THF. The reaction mixture was stirred for 24 h to give a dark purple solution. The solvent was removed under vacuum. The resulting solid was dissolved in hexane (10 mL), and the solvent was removed. Recrystallization of the product from ether at −35 °C over 2 days yielded $Ni_2(L^4)(COD)_2$ as purple crystals (19 mg, 0.018 mmol, 39% yield). ^{1}H NMR (C_6D_6, 400 MHz): δ 8.56 (s, 2H), 7.44 (t, J = 7.6, 2H), 7.40 (s, 4H), 7.33 (dd, J = 5.6, 1.2, 2H), 7.30 (s, 4H), 6.91 (dd, J = 6.8, 0.8, 2H), 5.57 (s, 4H), 3.90 (s, 8H), 3.06 (m, 4H), 2.97 (m, 2H), 2.67 (m, 4H), 1.62−1.50 (m, 8H), 1.27 (dd, J = 20.0, 6.4, 24H), 1.13 (d, J = 6.4, 12H). ^{13}C NMR (C_6D_6, 75 MHz): δ 161.68, 150.15, 149.04, 147.56, 146.03, 140.66, 138.12, 129.14, 128.85, 128.62, 128.14, 125.80, 125.35, 124.52, 121.50, 90.02, 83.10, 81.51, 66.28, 66.25, 35.53, 31.37, 31.20, 30.67, 30.52, 28.71, 27.50, 24.90, 22.01, 15.93. MS (ESI): calcd for $Ni_2(L^4)(COD)$ ($[C_{58}H_{74}N_4Ni_2]^+$) 942.4620, found 942.5277. Anal. Calcd for $C_{66}H_{86}N_4Ni_2$: C, 75.3; H, 8.2; N, 5.3. Found: C, 75.1; H, 8.0; N, 5.4.

$[Ni_2(L^1)_2]/[Ni_2(L^2)_2]/[Ni_2(L^1)(L^2)]$ (1b,c/2b,c/5b,c). A solution of L^2 (15 mg, 0.043 mmol) in toluene (5 mL) was added dropwise at room temperature to a stirred solution of $Ni_2(L^1)(COD)_2$ (30 mg, 0.046 mmol) in 5 mL of toluene. The reaction mixture was stirred for 2 h to give a purple solution. The solvent was removed under high vacuum. The resulting solid was dissolved in an additional 10 mL of THF, filtered, and dried in vacuo. The purple solid was washed with hexane (5 mL) and diethyl ether (5 mL) and dried to give the mixture of $Ni_2(L^1)_2$, $Ni_2(L^2)_2$, and $Ni_2(L^1)(L^2)$. ^{1}H NMR (C_6D_6, 400 MHz): $Ni_2(L^1)_2$ (isomer a), δ 10.17 (d, J = 5.6, 4H), 9.16 (s, 4H), 7.48−7.58 (m, 12H), 7.12 (s, 8H), 5.71 (d, J = 13.6, 4H), 4.85−5.0 (dd, J = 13.6, 10.0, 4H); $Ni_2(L^1)_2$ (isomer b), δ 10.14 (d, J = 4.8, 4H), 9.04 (s, 4H), 7.11 (s, 8H), 6.82−6.92 (m, 12H), 5.40 (d, J = 13.6, 4H), 4.85−5.0 (dd, J = 13.6, 10.0, 4H); $Ni_2(L^2)_2$ (isomer a), δ 10.36 (d, J = 6.0, 4H), 7.59 (m, 8H), 7.25 (s, 8H), 6.76 (d, J = 8.0, 4H), 6.58 (d, J = 14.4, 4H), 5.16 (d, J = 13.6, 4H), −0.41 (s, 12H); $Ni_2(L^2)_2$ (isomer b), δ 10.32 (d, J = 6.4, 4H), 7.57 (m, 8H), 6.97 (s, 8H), 6.48 (d, J = 8.0, 4H), 6.45 (d, J = 7.2, 4H), 5.09 (d, J = 13.6, 4H), −0.52 (s, 12H); $Ni_2(L^1)(L^2)$ (isomer a), δ 10.39 (d, J = 5.6, 2H), 10.28 (m, 2H), 9.20 (s, 2H), 7.48−7.31 (m, 12H), 7.27 (s, 4H), 7.04 (s, 4H), 5.66 (d, J = 12.8, 4H), 5.28 (d, J = 14.8, 4H), −0.34 (s, 6H); $Ni_2(L^1)(L^2)$ (isomer b), δ 10.26 (m, 2H), 10.23 (m, 2H), 9.19 (s, 2H), 7.48−7.31 (m, 12H), 7.09 (s, 4H), 4.84 (d, J = 13.2, 4H), 4.78 (d, J = 13.6, 4H), −0.51 (s, 6H). MS (ESI): calcd for $[Ni_2(L^2)_2]^+$ 800.3, found 800.3; calcd for $[Ni_2(L^1)(L^2)]^+$ 772.2, found 772.2; calcd for $[Ni(L^2)_2]^+$ 742.3, found 742.3; calcd for $[Ni(L^1)(L^2)]^+$ 714.3, found 714.3; calcd for $[Ni(L^1)_2]^+$ 686.2, found 686.3; calcd for $[Ni(L^2) + H]^+$ 401.1, found 401.2; calcd for $[Ni(L^1)]^+$ 372.1, found 372.3.

$Ni_2(L^2)(CS_2)_2$ (2d). A solution of L^2 (50 mg, 0.15 mmol) in 3 mL of THF was added at room temperature to a 3 mL solution of $Ni(COD)_2$ (80 mg, 0.29 mmol) in THF. The resulting mixture was stirred for 2 h. After that, CS_2 was added (0.29 mmol, 0.34 mL, 0.83 M in THF), causing precipitation of a purple solid, and the resulting mixture was stirred overnight. Purple solid was separated from the solution, washed with ether (10 mL), and dried to yield pure $Ni_2(L^2)(CS_2)_2$ (86 mg, 0.14 mmol, 94%). ^{1}H NMR (DMSO-d_6, 400 MHz): δ 9.50 (m, 2H), 8.24 (t, J = 8.0, 2H), 8.09 (d, J = 8.0, 2H), 7.89 (t, J = 6.4, 2H), 7.48 (s, 4H), 5.32 (s, 4H), 2.46 (s, 6H). ^{13}C NMR (DMSO-d_6, 75 MHz): δ 270.56 (corresponding to $^{13}CS_2$ in $Ni_2(L^2)(CS_2)_2$). MS (ESI): calcd for $Ni_2(L^2)(CS_2)$ ($[C_{23}H_{22}N_4Ni_2S_2 + H]^+$), 535.01 found 534.81. Anal. Calcd for $C_{24}H_{22}N_4Ni_2S_4$: C, 47.1; H, 3.6; N, 9.2. Found: C, 47.1; H, 3.7; N, 9.1.

$Ni_2(L^3)(CS_2)_2$ (3d). A suspension of L^3 (64 mg, 0.12 mmol) in 3 mL of THF was added at room temperature to a 3 mL solution of $Ni(COD)_2$ (65 mg, 0.24 mmol) in THF over the course of 1 h, and the reaction mixture was stirred for an additional 1 h. To the resulting purple solution was added CS_2 (0.095 mmol, 0.67 mL, 0.15 M in THF), leading to the formation of a dark precipitate. The reaction mixture was stirred for 12 h. Ether (10 mL) was added, and a dark brown solid was separated. The solid was washed with THF (15 mL) and ether (10 mL) and dried to afford $Ni_2(L^3)(CS_2)_2$ (49 mg, 0.064 mmol, 53% yield). ^{1}H NMR (DMF-d_7, 400 MHz): δ 8.62 (s, 2H), 8.17 (d, J = 8.0, 4H), 8.03 (m, 2H), 7.96 (m, 4H), 7.45 (s, 4H), 7.11 (d, J = 8.0, 4H), 4.94 (s, 4H), 3.89 (s, 6H). ^{13}C NMR (DMSO-d_6, 75 MHz): δ 264.41. Anal. Calcd for $C_{36}H_{30}N_4Ni_2O_2S_4$: C, 54.3; H, 3.8; N, 7.0. Found: C, 53.9; H, 3.5; N, 6.6.

$Ni_2(L^4)(CS_2)_2$ (4d). A suspension of L^4 (34 mg, 0.047 mmol) in 3 mL of THF was added at room temperature to a 3 mL solution of $Ni(COD)_2$ (26 mg, 0.095 mmol) in THF. To the resulting mixture was added CS_2 (0.095 mmol, 0.67 mL, 0.15 M in THF). The reaction mixture was stirred for 24 h to give a dark blue solution. The solvent was removed under vacuum. The resulting solid was washed successively with hexane (10 mL), ether (3 mL), and toluene (3 mL) and dried to afford $Ni_2(L^4)(CS_2)_2$ (22 mg, 0.022 mmol, 47%). ^{1}H NMR (DMSO-d_6, 400 MHz): δ 8.99 (s, 2H), 8.19 (t, J = 7.2, 2H), 7.95 (d, J = 8.0, 2H), 7.84 (d, J = 8.4, 2H), 7.45 (s, 4H), 7.07 (s, 4H), 5.40 (s, 4H), 2.91 (m, 2H), 2.24 (m, 4H), 1.15−1.25 (m, 24H), 1.00 (d, J = 8.0, 12H); ^{13}C NMR (DMSO-d_6, 75 MHz): δ 265.44 (also the peak for unbound $^{13}CS_2$ at δ 192.62 is due to decomposition of the product in DMSO-d_6). Anal. Calcd for $C_{52}H_{62}N_4Ni_2S_4$: C, 63.2; H, 6.3; N, 5.7. Found: C, 63.1; H, 6.2; N, 5.5.

Reaction of $Ni_2(L^2)(^{13}CS_2)_2$ (2d) with $(FeCp_2)(PF_6)$. A purple suspension of $Ni_2(L^2)(^{13}CS_2)_2$ (16 mg, 0.026 mmol) in 2 mL of

CD_3CN was treated at room temperature with a blue solution of $(FeCp_2)(PF_6)$ (1 equiv, 17 mg, 0.026 mmol) in CD_3CN (1 mL). The color changed to brown. The resulting mixture was stirred for 1 h. The reaction was followed by ^1H and ^{13}C NMR. The ^1H NMR (CD_3CN, 400 MHz) spectrum showed a single resonance attributable to $FeCp_2$ at δ 4.16. The ^{13}C NMR spectrum (CD_3CN, 75 MHz) showed two resonances, attributable to $^{13}CS_2$ and $Fe(C_5H_5)_2$, observed at δ 193.65 and 68.81 ppm, respectively.

Reaction of $Ni_2(L^2)(^{13}CS_2)_2$ with $CoCp^*_2$. The ^1H NMR (CD_3CN, 400 MHz) spectrum showed no peaks corresponding to $Ni_2(L^2)(^{13}CS_2)_2$ or $CoCp^*_2$. The ^{13}C NMR (CD_3CN, 75 MHz) spectrum demonstrated two resonances (δ 263.6 and 282.9 ppm) attributable to the ^{13}C-labeled carbons that originate in $^{13}CS_2$.

*$Ni_2(NHC)_2(CS_2)_2$ (**6**).* A purple suspension of $Ni_2(L^2)(CS_2)_2$ (66 mg, 0.11 mmol) in 2 mL of CD_3CN was treated at room temperature with 1,3-di-*tert*-butylimidazolin-2-ylidene (NHC, 40 mg, 0.22 mmol) in THF (1 mL). The mixture changed to red-brown. The resulting mixture was stirred for 2 h and filtered, and the volatiles were removed. The residue was extracted with THF (5 mL), and the solution was concentrated to ca. 1 mL and layered with ether (10 mL). Recrystallization overnight at −33 °C formed $Ni_2(NHC)_2(CS_2)_2$ as purple crystals (24 mg, 0.038 mmol, 35% yield). ^1H NMR (C_6D_6, 400 MHz): δ 6.51 (s, 2H), 1.69 (s, 18H). ^{13}C NMR (C_6D_6, 400 MHz, $^{13}CS_2$-labeled sample): δ 283.51. Anal. Calcd for $C_{24}H_{40}N_4Ni_2S_4{\cdot}C_4H_8O$: C, 47.9; H, 6.9; N, 8.0. Found: C, 47.6; H, 6.6; N, 8.8.

X-ray Crystallographic Details. Structures of compounds **2d**, **3b**, **4a**,**b**, **6**, and L^2 were confirmed by X-ray analysis; the structures of **1d** and **2b**,**c** were previously reported. Table S1 (Supporting Information) presents selected structural and refinement data for compounds L^2, **2d**, **3b**, **4a**,**b**, and **6**. The crystals were mounted on a Bruker APEXII/Kappa three-circle goniometer platform diffractometer equipped with an APEX-2 detector. A graphic monochromator was employed for wavelength selection of the Mo Kα radiation (λ = 0.71073 Å). The data were processed and refined using the program SAINT supplied by Siemens Industrial Automation. Structures were solved by direct methods in SHELXS and refined by standard difference Fourier techniques in the SHELXTL program suite (version 6.10, G. M. Sheldrick and Siemens Industrial Automation, 2000). Hydrogen atoms were placed in calculated positions using the standard riding model and refined isotropically; all other atoms were refined anisotropically. The asymmetric units of L^2, **4a**, and **6** contain only half of the centrosymmetric molecule. The structure of **3b** was of somewhat low quality due to the poorly diffracting crystals. The structure contained two methoxy groups that were found to be disordered over two positions. The disorder was satisfactorily modeled. In addition, the structure contained one hexane molecule per asymmetric unit. The structure of **4a** contained one ether molecule. The structure of **4b** contained three partially disordered solvent molecules that were modeled as hexane (crystallization solvent) with partial occupancies. The structure of **2d** was of very low quality due to the small crystal size, poor diffraction, and twinned nature of the crystals. Therefore, only the overall connectivity and the approximate metal−metal separation of **2d** are discussed in the paper.

■ RESULTS AND DISCUSSION

Ligand Synthesis and Characterization. To evaluate steric and electronic effects in the bis(iminopyridine) framework, we have synthesized ligands L^1−L^7 (Figure 1). Electronic effects in the iminopyridine chelate were manipulated via substitution at two positions: the imino carbon position and the pyridine 2′ (ortho)-position. Steric effects were evaluated by employing various bulky groups at the pyridine 2′-position. L^1 is a prototypical ligand featuring hydrogens only. L^2 has methyl groups at the imino carbons. L^3 and L^5 bear bulky electron-rich 4-methoxyphenyl and bulky electron-withdrawing 4-cyanophenyl groups at the pyridine 2′-position, respectively. L^4 has very bulky 2,4,6-triispropylphenyl groups at the pyridine 2′-position while L^6 and L^7 feature more compact, electronically diverse substituents at the 2′-position of the pyridine: the electron-rich OMe group and the electron-withdrawing CF_3 group, respectively. L^1 and L^2 have been previously reported, by us and others,[10,13] while L^3−L^7 have not been previously synthesized. The synthesis of L^1−L^7 was accomplished by the reflux of 2 equiv of the respective aldehyde/ketone with 1,4-phenylenedimethanamine. All the aldehydes were obtained commercially except for 6-(2,4,6-triisopropylphenyl)-picolinaldehyde. This aldehyde was prepared as described in Figure 2. We have also attempted to synthesize L^8, that features

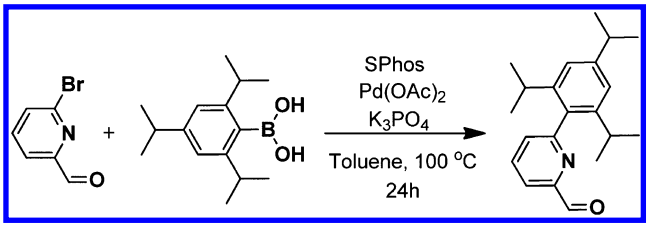

Figure 2. Synthesis of 6-(2,4,6-triisopropylphenyl)picolinaldehyde.

an electron-withdrawing CF_3 group at the imino carbon position. However, although ligand formation occurs after prolonged reflux, we were not able to isolate it in a pure form. Therefore, this ligand will not be discussed.

The ligands were characterized by ^1H, $^{13}C\{^1H\}$ (^{13}C thereafter), and ^{19}F (where applicable) NMR spectroscopy and by high-resolution mass spectrometry (HRMS); the spectra can be found in the Supporting Information. L^2 was also characterized by X-ray crystallography (Figure S1, Supporting Information). The structure of L^2 (alongside the previously reported structure of L^1)[13a] provides information about the carbon−nitrogen (C4−N2, 1.275(4) Å) and the carbon−carbon (C3−C4, 1.496(5) Å) bond distances unperturbed by bound metals and therefore serves to calibrate redox effects on the iminopyridine chelate. As in the structure of L^1, L^2 displays an *anti* conformation for the nitrogens of the imine and the pyridine. The two sides of the ligands are also *anti*.

The ligand precursors were characterized by cyclic voltammetry (see section 5 of the Supporting Information for details). Figure 3 shows the cyclic voltammograms (CVs) of the ligand precursors in DMF (except for L^4, due to insufficient solubility). The ligands' CVs exhibit two irreversible reduction waves at potentials higher than −2.3 V. Following the cathodic sweep, an irreversible oxidation is observed between −1.5 and −1.1 V depending on the ligand. Comparison of the reduction potentials of the ligands with sterically similar, but electronically diverse, substituents indicates that the ligands possessing electron-withdrawing groups are somewhat easier to reduce. Thus, the first reduction of L^1 peaks at −2.4 V (onset at −2.1 V), whereas for L^2 the corresponding potential is −2.7 V (onset at −2.4 V). Such a difference may explain the disparity in the reactivity of these sterically comparable ligands with $Ni(COD)_2$: whereas L^1 undergoes fast reaction with $Ni(COD)_2$ that forms $Ni_2(L^1)(COD)_2$, the reaction of L^2 is significantly slower and results in the formation of $Ni_2(L^2)_2$ species. Other ligands (L^5 vs L^3, L^7 vs L^6) display an overall similar trend, although ortho substitution results in less pronounced changes in the reduction potential.

Synthesis of the $Ni_2(L)(COD)_2$ and $Ni_2(L)_2$ Complexes. Figure 4 summarizes the syntheses and the reactivity of the

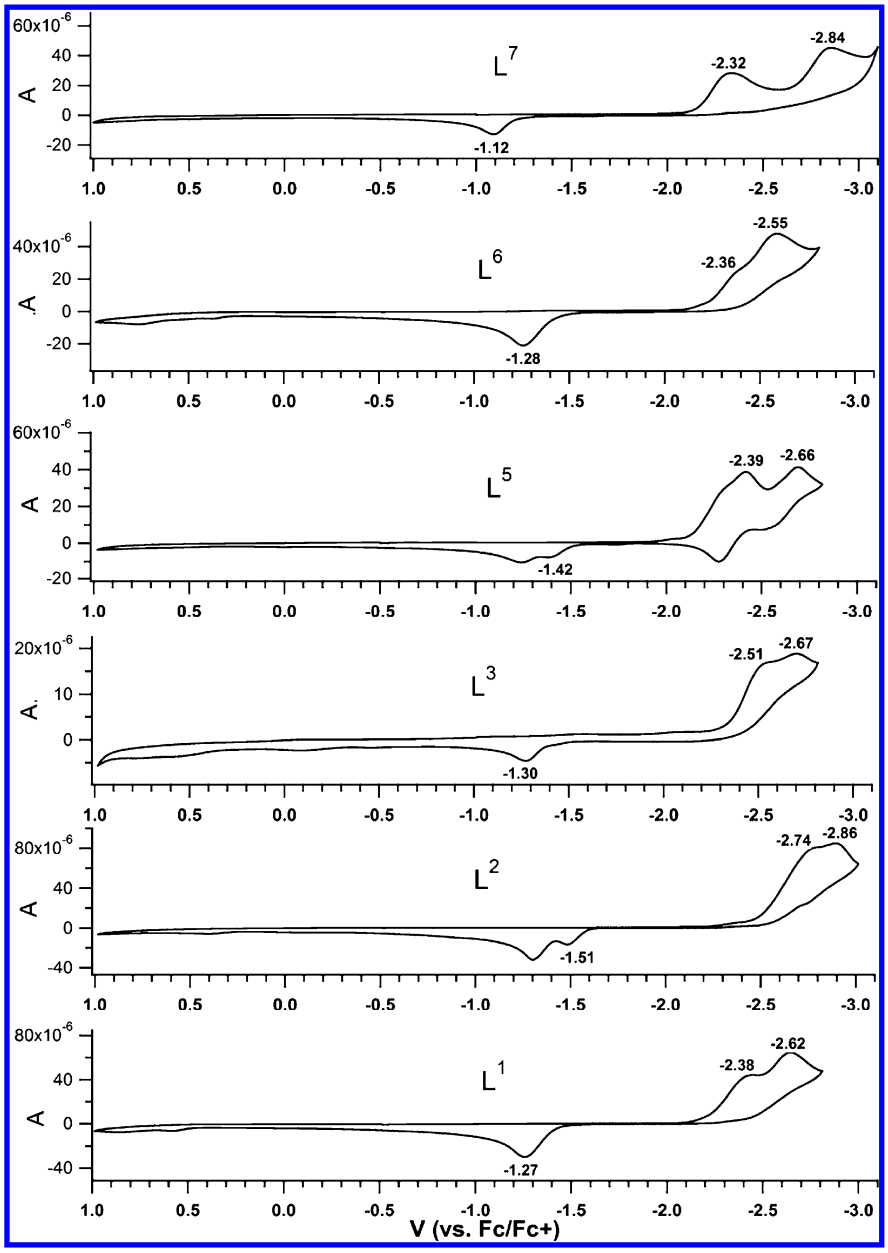

Figure 3. Cyclic voltammograms of L^1–L^3 and L^5–L^7 ligand precursors in DMF (0.1 M $[NBu_4](PF_6)$ supporting electrolyte, 25 °C, platinum working electrode, 100 mV/s scan rate).

metal compounds described in this paper; the abbreviations are shown in Table 1. Treatment of L^1 with 2 equiv of $Ni(COD)_2$ leads cleanly to the formation of $Ni_2(L^1)(COD)_2$ (**1a**) in 63% yield, whereas treatment of L^1 with 1 equiv of $Ni(COD)_2$ forms $Ni_2(L^1)_2$ (**1b**,**c**).[10a] In contrast, treatment of L^2 with either 1 or 2 equiv of $Ni(COD)_2$ invariably forms the bis(homoleptic) complex $Ni_2(L^2)_2$ (**2b**,**c**). Since both ligands feature similar steric parameters, we postulated that the origin of the difference in their reactivity is electronic: the Me group in the imino carbon position creates a relatively electron-rich iminopyridine chelate. To further evaluate the impact of the electronic effects on L reactivity, we compared the reactivity of L^3 and L^5. L^3 and L^5 both contain comparatively bulky, but electronically diverse, *p*-methoxyphenyl and *p*-cyanophenyl groups at the 2′-position of the pyridine. L^5 failed to lead to an isolable product, presumably undergoing activation of the cyano group at Ni(0). The electron-rich and more robust L^3, on the other hand, led cleanly to the formation of the bis(homoleptic) complexes $Ni_2(L^3)_2$ (**3b**,**c**), independent of the ligand-to-metal ratio. NMR of the crude product contained only species attributable to $Ni_2(L^3)_2$ and $Ni(COD)_2$, implying that no other products were formed. The product can be recrystallized from THF/ether at −40 °C to give brown crystals of $Ni_2(L^3)_2$ in 60% yield. Next, we compared the reactivity of L^6 and L^7, featuring an electron-rich and electron-withdrawing OMe and CF_3 group at the pyridine 2′-position. The crude reaction mixture of L^6 with 2 equiv of $Ni(COD)_2$ indicated the presence of the bis(homoleptic) complexes. However, the products were not stable and could not be isolated. L^7 underwent fast reaction with $Ni(COD)_2$, as indicated by an immediate color change to violet. However, it failed to form either $Ni_2(L)(COD)_2$ or $Ni_2(L)_2$ species. Instead, it forms different diamagnetic products whose natures are still elusive to us. Finally, L^4 tested mostly the steric effect, featuring 2,4,6-triisopropylphenyl

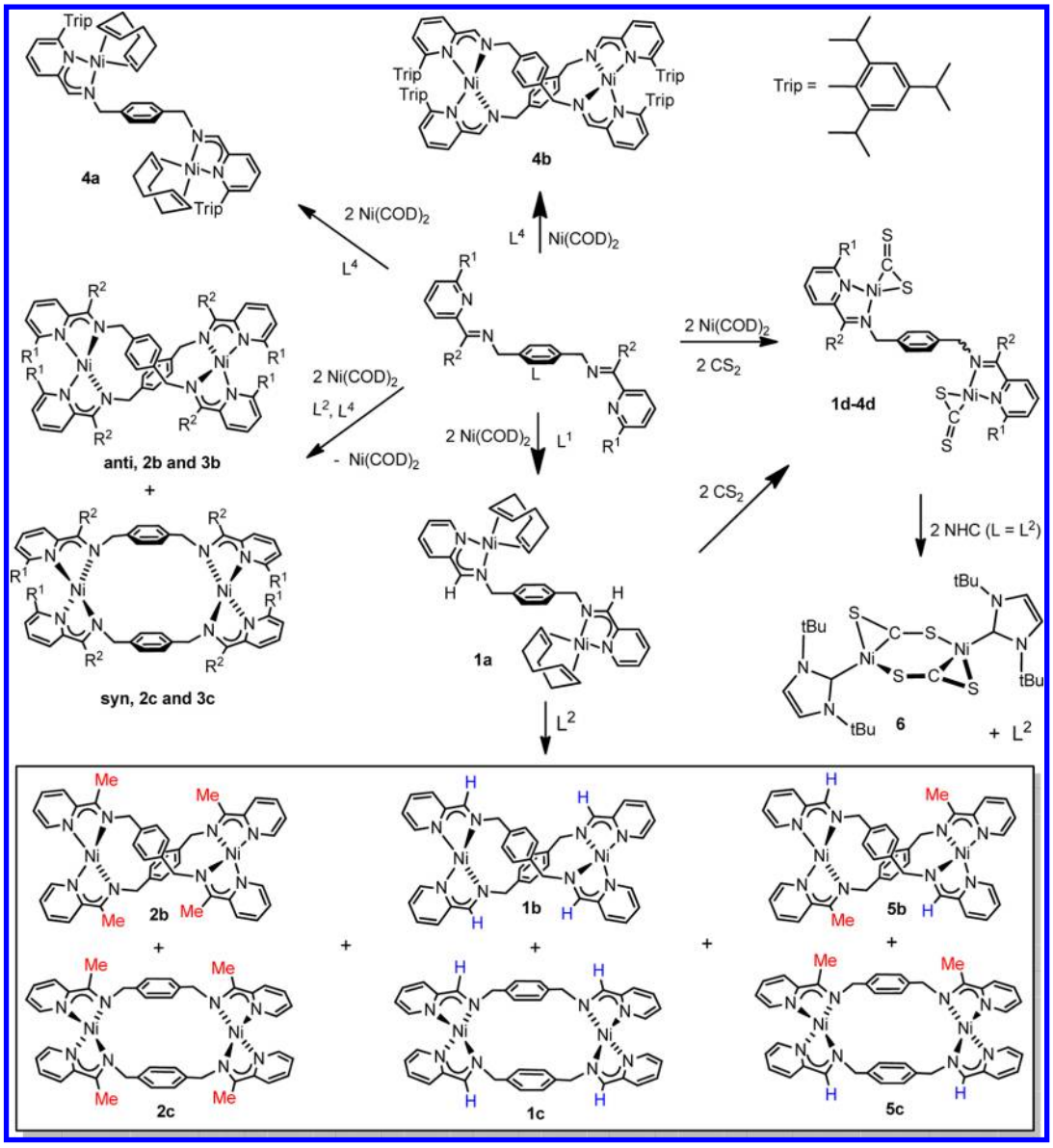

Figure 4. Schematic representation of the synthetic routes toward the dinickel compounds described in this paper.

Table 1. Designation of Compounds and Their Abbreviation

$Ni_2(L^1)(COD)_2$	**1a**
syn-$Ni_2(L^1)_2$	**1b**
anti-$Ni_2(L^1)_2$	**1c**
$Ni_2(L^1)(CS_2)_2$	**1d**
syn-$Ni_2(L^2)_2$	**2b**
anti-$Ni_2(L^2)_2$	**2c**
$Ni_2(L_2)(CS_2)_2$	**2d**
syn-$Ni_2(L^3)_2$	**3b**
anti-$Ni_2(L^3)_2$	**3c**
$Ni_2(L^3)(CS_2)_2$	**3d**
$Ni_2(L^4)(COD)_2$	**4a**
$Ni_2(L^4)_2$	**4b**
$Ni_2(L^4)(CS_2)_2$	**4d**
syn-$Ni_2(L^1)(L^2)$	**5b**
anti-$Ni_2(L^1)(L^2)$	**5c**
$Ni_2(NHC)_2(CS_2)_2$	**6**

groups at the 2′-position of the pyridine. The presence of the bulky groups leads to a well-behaved reactivity of the ligand with $Ni(COD)_2$. Slow addition of L^4 to 2 equiv of $Ni(COD)_2$ in toluene forms mostly $Ni_2(L)(COD)_2$, on the basis of the NMR spectrum of the resulting product. Pure $Ni_2(L^4)(COD)_2$ was obtained by recrystallization from ether and isolated as purple crystals in 39% yield. Its structure was confirmed by X-ray crystallography. Treatment of L^4 with 1 equiv of $Ni(COD)_2$ forms mostly the bis(homoleptic) complex $Ni_2(L^4)_2$. $Ni_2(L^4)_2$ was obtained by recrystallization from hexane at −40 °C as blue-violet crystals in 27% yield, and its structure was also verified by X-ray crystallography. In addition, its purity was confirmed by elemental analysis. $Ni_2(L^4)_2$ is unstable in solution: analytically pure samples of $Ni_2(L^4)_2$ in C_6D_6 demonstrate progressive disappearance of the $Ni_2(L^4)_2$-attributed signals coupled with the increase in the intensity of free ligand signals. After eight hours at room temperature, ca. 30% of the complex remains.

Spectroscopic and Electrochemical Characterization of the $Ni_2(L)(COD)_2$ and $Ni_2(L)_2$ complexes. The complexes were characterized by NMR spectroscopy and mass spectrometry. Two isolated $Ni_2(L)(COD)_2$ complexes (**1a** and **4a**) both

display C_{2v}/C_{2h} symmetry on the NMR time scale at room temperature: one set of signals is observed for both arms of the dinuclear system, the protons of the central benzene ring appear as a singlet, and the methylene bridge protons give rise to a singlet as well. COD protons, on the other hand, appear as three multiplets (broad signals are observed for **4a**). Such a spectrum is consistent with the complex constantly residing in either the syn (C_{2v}), or the anti (C_{2h}) conformation or undergoing fast equilibration between *syn* and *anti* conformations (see below for DFT calculations of the stability of different conformers of $Ni_2L(COD)_2$ species). The lack of symmetry at a given Ni center causes COD signals to appear as three multiplets. $Ni_2(L)_2$ complexes, on the other hand, demonstrate AB signals for the methylene benzyl signals, being consistent with restricted rotation around the benzyl methylene bond. Two stereoisomers are observed in NMR spectra of the $Ni_2(L^2)_2$ and $Ni_2(L^3)_2$ complexes **2b,c** and **3b,c**. On the basis of the crystal structure of $Ni_2(L^2)_2$,[10a] we previously correlated these stereoisomers with the *syn* and *anti* isomers. A single stereoisomer is observed for $Ni_2(L^4)_2$ (**4b**), possibly as a result of steric pressure that makes the *syn* isomer unstable. Molecular ions $[Ni_2(L)_2]^+$ are observed in the mass spectra of all the $Ni_2(L)_2$ compounds. For $Ni_2(L)(COD)_2$ compounds, the molecular ions appear to be unstable under ionizing conditions and are detected only at a very low intensity. Interestingly, $[Ni_2(L)(COD)]^+$ compounds are observed at significantly higher intensities.

Cyclic voltammograms of the homoleptic complexes $Ni_2(L)_2$ (L = L^1, L^2, L^3) demonstrate similar features. Figure 5 shows

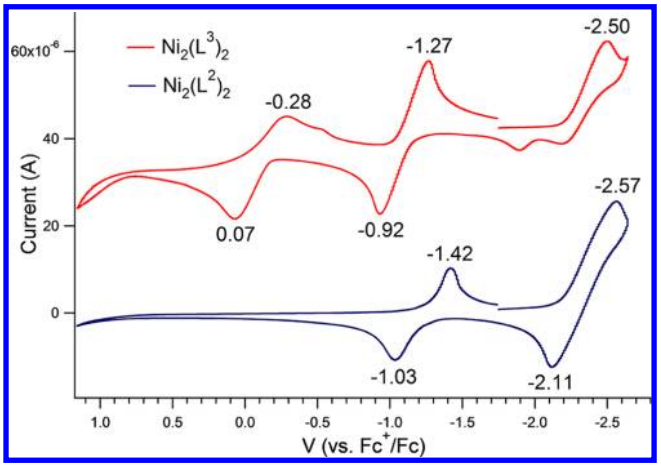

Figure 5. Cyclic voltammogram of $Ni_2(L^2)_2$ and $Ni_2(L^3)_2$ in THF (0.1 M $[NBu_4](PF_6)$, 25 °C, platinum working electrode, 100 mV/s scan rate).

CVs of $Ni_2(L^2)_2$ and $Ni_2(L^3)_2$ complexes. Cyclic voltammetry of all species demonstrates reduction (between −2.3 and −2.6 V) and reversible oxidation (−1.1 to −1.2 V). Comparison of these results with the electrochemical studies on the mononuclear bis(iminopyridine)Ni complex[11a] suggests that these events are ligand-based. Wieghardt and co-workers have observed an additional reversible peak at −0.57 V for the mononuclear bis(iminopyridine)Ni complex,[11a] which was attributed to the metal-centered oxidation (Ni^{II}/Ni^{I}). In our complexes, an additional oxidation is observed for the $Ni_2(L^3)_2$ complex only. The $Ni_2(L)(COD)_2$ complexes show similar redox properties (see the Supporting Information for details). One reduction and two oxidation events are observed. However, $Ni_2(L)(COD)_2$ complexes demonstrate broader peaks, presumably due to the conformational lability of these complexes.

Ligand Lability As Demonstrated by the Reaction of $Ni_2(L^1)(COD)_2$ with L^2. We have previously interrogated the nature of the L binding to the Ni centers by theoretical methods. DFT calculations demonstrated that each iminopyridine unit has a $^1/_2-$ charge in the bis(homoleptic) complexes of the $Ni_2(L)_2$ type.[10a] This finding implies that the ligand should be relatively labile. We decided to probe the lability of the bis(iminopyridine) ligand by a ligand competition experiment. We treated the $Ni_2(L^1)(COD)_2$ complex with 1 equiv of L^2. We postulated that if L^1 is strongly bound to Ni as a 1− ligand, then the reaction should lead cleanly to the formation of $Ni_2(L^1)(L^2)$. Labile binding, on the other hand, should result in the formation of a mixture of products. The reaction outcome was analyzed by NMR spectroscopy and mass spectrometry (MS). NMR and MS both indicate that the formation of all possible products takes place. The ^{1}H NMR spectrum displays features consistent with the previously characterized $Ni_2(L^1)_2$ and $Ni_2(L^2)_2$ compounds (see the Supporting Information for details). It addition, it contains signals attributable to the *syn* and *anti* isomers of the mixed-ligand product, $Ni_2(L^1)(L^2)$. The mass spectrum provides further indication for the proposed mixture of products (Figure 6). The spectrum displays three

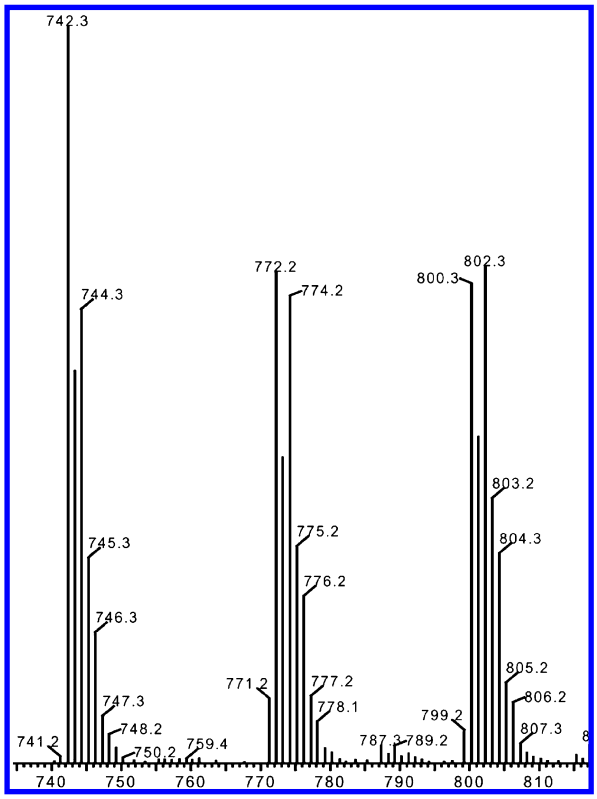

Figure 6. Mass spectrum of the reaction products $[Ni(L^2)_2]$, $[Ni_2(L^1)(L^2)]$, and ($[Ni_2(L^1)_2]$ + $[Ni(L^1)_2]$).

intense peaks. The peak at m/z 800.2 agrees with the predicted spectrum for $Ni_2(L^2)_2^+$, and the peak at m/z 772 corresponds to $Ni_2(L^1)(L^2)^+$. The peak at m/z 742.3 may correspond to the $[Ni_2(L^1)(L^2) - 2H]^+$ species or to the overlap of the mono-Ni $Ni(L^2)_2^+$ species (m/z 742.3) and $Ni_2(L^1)_2^+$ (m/z 744.3).

Structures of the $Ni_2(L)_2$ and $Ni_2L(COD)_2$ Complexes. Selected compounds were characterized by X-ray crystallog-

raphy. The structures are presented in Figures 7–9, and the relevant bond distances and angles are tabulated in Table 2.

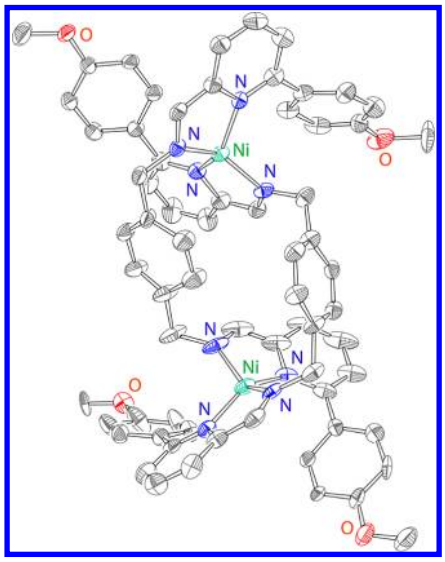

Figure 7. Structure of $Ni_2(L^3)_2$ (**3b**), with 30% probability ellipsoids.

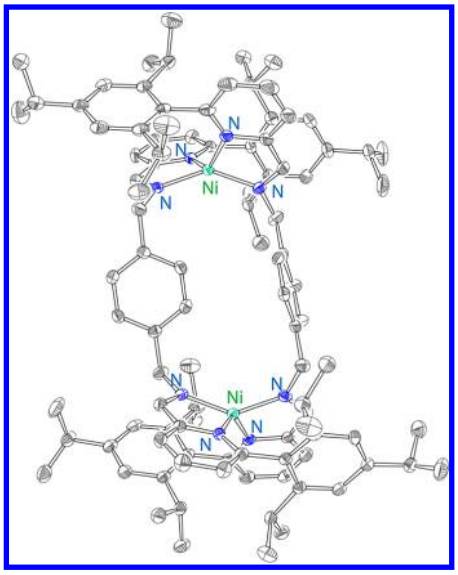

Figure 8. Structure of $Ni_2(L^4)_2$ (**4b**), with 50% probability ellipsoids.

The structures of the bis(homoleptic) $Ni_2(L^3)_2$ and $Ni_2(L^4)_2$ complexes are precedented by the structure of $Ni_2(L^2)_2$ (that is also included in Table 2). Unlike the structure of $Ni_2(L^2)_2$, which contained two stereoisomers, $Ni_2(L^3)_2$ exists as a single stereoisomer in the solid state (Figure 7). Dissolution of the crystals in C_6D_6 solution re-forms two stereoisomers. A single solid-state isomer of $Ni_2(L^4)_2$ (Figure 8) is consistent with a single isomer in solution. The structure of $Ni_2(L^4)(COD)_2$ (**4a**) represents the first example of a crystallographically characterized bis(COD) complex in our system (Figure 9). The two parts of the dinuclear complex are in the *anti* conformation, and the Ni centers are in an approximately tetrahedral geometry. Several trends can be discerned from Table 2. Whereas the Ni–N(imine) bonds are unaffected by the steric bulk of the iminopyridine chelate, Ni–N(pyridine) bonds gradually increase upon an increase in the steric bulk of the pyridine 2′-substituent. Similarly, the dihedral angle between

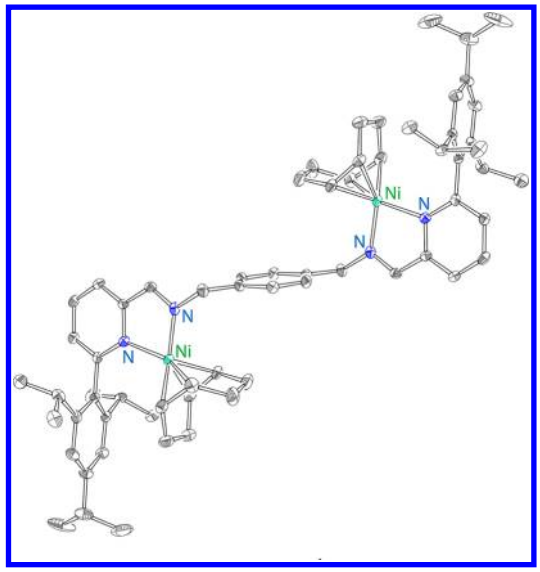

Figure 9. Structure of $Ni_2(L^4)(COD)_2$ (**4a**), with 50% probability ellipsoids.

Table 2. Selected Bond Distances (Å) and Angles (deg)

	C=N[a]	C–C[a]	IP–Ni–IP[b]	Ni–N_{im}	Ni–N_{py}
2b,c	1.331(3)	1.426(4)	52(2)	1.908(3)	1.921(5)
3b	1.31(1)	1.39(1)	63(3)	1.89(1)	1.95(1)
4b	1.314(3)	1.415(3)	69 (1)	1.906(4)	1.999(9)
4a	1.309(3)	1.422(3)		1.925(2)	2.008(2)
L^2	1.275(4)	1.496(5)			
L^1	1.256(2)	1.472(2)			

[a]Average and standard deviation of all the relevant distances. [b]Average and standard deviation of (NCCN)–Ni–(NCCN) dihedral angle.

the iminopyridine planes increases for the bulkier groups. A comparison of the C=N and C–C bond distances in the metal complexes with the corresponding distances in L^1 and L^2 clearly indicates substantial reduction of the iminopyridine unit.[11]

Synthesis and Structures of the $Ni_2(L)(CS_2)_2$ Complexes. We have previously reported that the reaction of $Ni_2(L^1)(COD)_2$ with 2 equiv of carbon disulfide forms $Ni_2(L^1)(CS_2)_2$ (**1d**) in high yield.[10b] We were not able to isolate $Ni_2(L)(COD)_2$ for other ligands (except for L^4). However, $Ni_2(L)_2$ complexes were shown to be labile in solution and the reaction of $Ni_2(L^2)_2$ with diphenylacetylene (DPA) was demonstrated to form $Ni_2(L)(DPA)_2$ as one of the products.[10a] On the basis of these observations, we surmised that combining $Ni(COD)_2$, L, and CS_2 may still form the desired product. Gratifyingly, the addition of 2 equiv of carbon disulfide to a mixture of $Ni(COD)_2$ (2 equiv) and L^2 led to the formation of bright purple $Ni_2(L^2)(CS_2)_2$ (**2d**; 94% yield). A similar protocol formed purple-brown $Ni_2(L^3)(CS_2)_2$ (**3d**; 53% yield) and blue $Ni_2(L^4)(CS_2)_2$ (**4d**; 47% yield).

These CS_2 complexes were characterized by ^1H and ^{13}C NMR spectroscopy, mass spectrometry, and elemental analysis. ^{13}C NMR spectra of the $^{13}CS_2$-labeled samples display a resonance around 267 ppm that is characteristic of the metal-bound CS_2 group.[6,10] In addition, the structure of $Ni_2(L^2)(CS_2)_2$ (**2d**) has been confirmed by an X-ray structure determination. The structure of **2d** is of low quality, but it clearly demonstrates the connectivity pattern and the positions of the two metal centers. Figure 10 displays the structure of **2d**, along with the previously reported structure of **1d**.[10b] Both

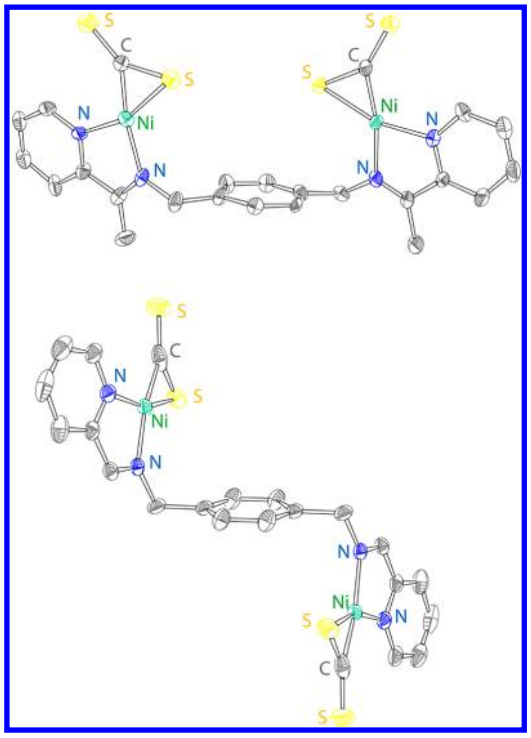

Figure 10. Structures of the bimetallic CS_2 complexes $Ni_2(L^1)(CS_2)_2$ (**1d**, top) and $Ni_2(L^2)(CS_2)_2$ (**2d**, bottom).

structures contain two distorted-square-planar nickel(II) centers each coordinating side-on-bound carbon disulfide. Whereas the structure of **1d** had an *anti* conformation of the two CS_2-bound nickel centers, the heteroallene adducts in **2d** are *syn*. Accordingly, $C(CS_2)$- - -$C(CS_2)$ separations are 11.2 Å for the *anti* (**1d**) species and 7.6 Å for the *syn* (**2d**) structure. This finding provides crystallographic evidence that the two heteroallenes bound by the bis(iminopyridine) dinickel system can be in the vicinity of each other.

Electrochemistry of CS_2 Complexes. $Ni_2(L)(CS_2)_2$ complexes were characterized by cyclic voltammetry. CVs of **1d**, **2d**, and **4d** are presented in Figure 11. We were not able to obtain a reliable CV of **3d**, due to its extremely low solubility. In the cathodic sweep, two ligand-based reduction events are observed for all of the complexes: a quasi-reversible reduction, followed by an irreversible reduction. The overall pattern of the electrochemical events described for **1d**, **2d**, and **4d** is similar to that for the $Ni_2(L)_2$ and $Ni_2(L)(COD)_2$ complexes. The characteristic difference is that the first reversible event is a reduction in the case of $Ni_2(L)(CS_2)_2$ complexes but an oxidation for the $Ni_2(L)_2$ and $Ni_2(L)(COD)_2$ complexes. This difference results from the fact that the iminopyridine unit is fully oxidized in $Ni_2(L)(CS_2)_2$,[10b] but partially reduced in $Ni_2(L)_2$ and $Ni_2(L)(COD)_2$.[10a] In addition, an irreversible oxidation event is observed in all the $Ni_2(L)(CS_2)_2$ complexes. As the only possible location for the oxidation event is at the η^2-bound CS_2, we postulated that an oxidation of the reduced carbon disulfide leads to a chemical transformation.

Reactivity of CS_2 Complexes. Following the electrochemical experiments, we carried out chemical oxidation and reduction. For that purpose, we decided to use $Ni_2(L^2)(^{13}CS_2)_2$ complexes: this complex has higher solubility than previously studied $Ni_2(L^1)(^{13}CS_2)_2$ or $Ni_2(L^3)(^{13}CS_2)_2$, and ^{13}C-labeled carbon disulfide enables convenient monitoring of the reaction by ^{13}C NMR spectroscopy. Oxidation of $Ni_2(L^2)(^{13}CS_2)_2$ in

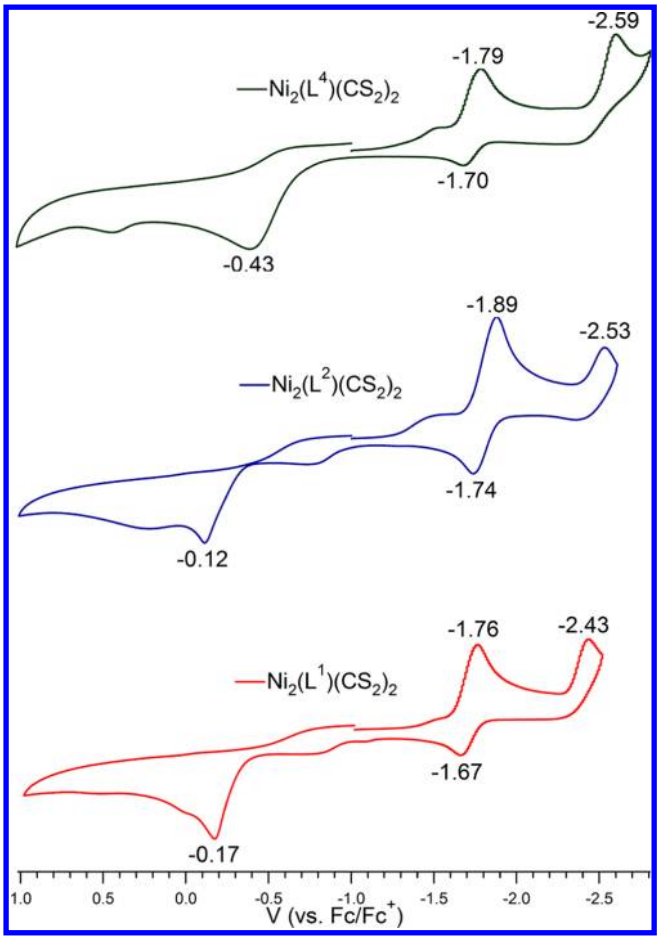

Figure 11. Cyclic voltammograms of $Ni_2(L^1)(CS_2)_2$, $Ni_2(L^2)(CS_2)_2$, and $Ni_2(L^4)(CS_2)_2$ in DMF (0.1 M $[NBu_4](PF_6)$ supporting electrolyte, 25 °C, platinum working electrode, 100 mV/s scan rate).

CD_3CN with 2 equiv of $(FeCp_2)(OTf)$ forms $FeCp_2$ and liberates $^{13}CS_2$. No free ligand was observed by NMR spectroscopy, suggesting that the $[Ni_2(L)]$ fragment remains intact. These findings are consistent with our previous report on the oxidation of $Ni_2(L^1)(^{13}CS_2)_2$ in DMSO.[10b] Reduction of $Ni_2(L^2)(^{13}CS_2)_2$ in CD_3CN with 2 equiv of $Co(Cp^*)_2$ leads to the formation of $[Co(Cp^*)_2]^+$ (identified by NMR spectroscopy) and the formation of a new ^{13}C NMR signal at 283 ppm. We were not able to identify the nature of the resulting Ni product.

We have also investigated the reaction of $Ni_2(L^2)(^{13}CS_2)_2$ with N-heterocyclic carbene. Addition of 2 equiv of NHC (NHC = 1,3-di-*tert*-butylimidazolin-2-ylidene) to a stirred suspension of **2d** forms a purple-pink solution. Recrystallization of the residue from THF/ether at −40 °C leads to the isolation of **6** in ca. 40% yield. The ^1H NMR spectrum of the product contains two resonances (both singlets) attributable to the NHC protons. The ^{13}C NMR spectrum contains a new $^{13}CS_2$ resonance at 283 ppm. X-ray structure determination reveals a $[Ni_2(\mu_2\text{-}CS_2)_2]$ core supported by NHC ligands (Figure 12). The topology of the core has been precedented for the phosphine ligands[14] but has not been isolated for the N-heterocyclic carbenes. Compound **6** demonstrates the shortest distance between the CS_2 carbons (3.15 Å) obtained so far in our research, and we are investigating its electronic structure and reactivity. It is worth noting that the reaction of $Ni(COD)_2$ with NHC and CS_2 in the absence of L^2 forms a mixture of two

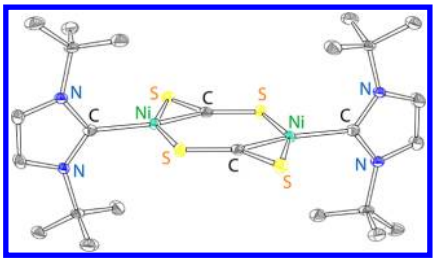

Figure 12. X-ray structure of **7**, with 50% probability ellipsoids.

compounds, one of them being **6** (see Figures S41 and S42 in the Supporting Information). Therefore, the dinucleating ligand L^2 provides a template for the clean formation of the dinuclear complex **6**.

DFT Calculations. To evaluate the possible thermodynamic influence of ligand substituents on the reactivity of these bis(iminopyridine) complexes, we evaluated the thermodynamics of COD substituting one iminopyridine using density functional theory (see section 7 of the Supporting Information for details):

$$[Ni(L^m)_2] + COD \leftrightarrows [Ni(L^m)(COD)] + L^m$$

Five ligands were studied: L^{1m} with $R_1 = R_2 = H$, L^{2m} with $R_1 = H$, $R_2 = Me$, L^{3m} with $R_1 = H$, $R_2 = CF_3$, L^{4m} with $R_1 = Me$, $R_2 = H$, and L^{5m} with $R_1 = CF_3$, $R_2 = H$ (see Figure 13). These

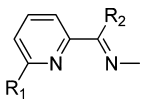

Figure 13. Model ligands with substituents.

data represent both electron-donating and -withdrawing groups at the 2′-position of pyridine (L^{4m}/L^{5m}) and the imine carbon (L^{2m}/L^{3m}). A summary of the thermodynamics is included in Table 3. The displacement of an iminopyridine by COD is

Table 3. Thermodynamics of Ligand Exchange Predicted by DFT

reaction	energy (kcal/mol)
$[Ni(L^{1m})_2] + COD \leftrightarrows [Ni(L^{1m})(COD)] + L^{1m}$	17.01
$[Ni(L^{2m})_2] + COD \leftrightarrows [Ni(L^{2m})(COD)] + L^{2m}$	19.03
$[Ni(L^{3m})_2] + COD \leftrightarrows [Ni(L^{3m})(COD)] + L^{3m}$	17.09
$[Ni(L^{4m})_2] + COD \leftrightarrows [Ni(L^{4m})(COD)] + L^{4m}$	18.68
$[Ni(L^{5m})_2] + COD \leftrightarrows [Ni(L^{5m})(COD)] + L^{5m}$	18.87

predicted to be unfavorable for each bis(iminopyridine) complex. However, the least unfavorable reaction is for the ligand with hydrogens at R_1 and R_2, which is most similar to the experimental ligand L^1. Both of the ligands with imine substituents show less favorable displacement by COD and the bis(iminopyridine) compounds show a noticeably longer $C_{pyr}-C_{im}$ bond length of ~1.45 (L^{2m}/L^{3m}) vs 1.43 Å (L^{1m}). Thus, any substituent that provides polarizability for the radical iminopyridine anion[10a] seems to disfavor formation of the COD complex. The pyridyl substituents do not show a simple trend in the ligand displacement thermodynamics (L^{4m}/L^{5m}). These structures demonstrate much larger interligand dihedral angles due to the steric conflicts of the substituents. These sterics influence the ligand exchange thermodynamics in a nontrivial way.

We also explored the thermodynamics of various conformers of the dinuclear species $Ni_2(L)(COD)_2$ and $Ni_2(L)(CS_2)_2$. Details of these calculations are included in the Supporting Information, but we find no significant thermodynamic difference between the *syn* and *anti* conformers. This was expected for the bis-CS_2 complex, since both the *syn* and *anti* conformers were observed crystallographically. We speculated that the $Ni_2(L)(COD)_2$ complexes could experience steric conflicts in the *syn* conformer, since only the *anti* conformer was observed crystallographically. As Figure 14 demonstrates,

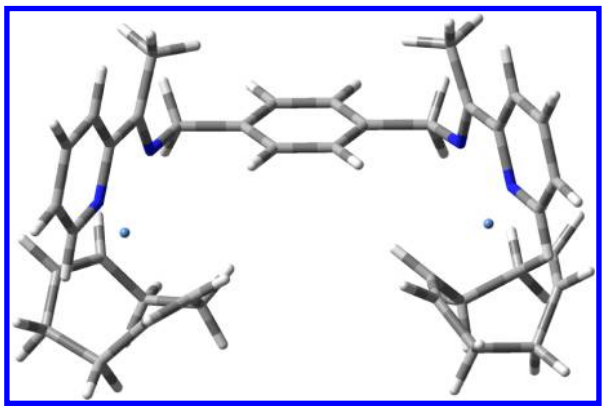

Figure 14. Image of the lowest energy *syn* conformer of $Ni_2(L^2)(COD)_2$.

however, there is sufficient flexibility in the bis(iminopyridine) ligands for the Ni-COD moieties to avoid one another. The Ni centers are well separated at 8.49 Å. The closest COD H···H separation occurs at 4.24 Å. This *syn* complex is computed to be 0.55 kcal/mol more stable than the lowest energy *anti* conformer. Within the limits of our DFT methodology this energy difference is insignificant and suggests that the observation of only the *anti* conformer experimentally may have more to do with packing effects than an intrinsic stability of one conformer vs the other.

■ SUMMARY AND CONCLUSIONS

In the present study we investigated (i) steric and electronic effects in the formation of $Ni_2(L)(COD)_2$ complexes vs $Ni_2(L)_2$, (ii) properties and the L ligand lability in the resulting species, (iii) formation, structures, and electrochemical properties of the $Ni_2(L)(CS_2)_2$ complexes, (iv) reactivity of the $Ni_2(L)(CS_2)_2$ complexes. Reactivity studies disclose that ligands featuring electron-donating groups react more slowly with $Ni(COD)_2$ and lead preferentially to the formation of $Ni_2(L)_2$ complexes. DFT calculations agree with the conclusion that the electron-withdrawing groups in the imine position provide some stabilization to Ni(L)(COD) complexes vs $Ni_2(L)_2$ complexes. Structural and theoretical data for $Ni_2(L)(COD)_2$ are consistent with the free rotation of the ligand chelating units vs each other. We also discovered that prior isolation of $Ni_2(L)(COD)_2$ complexes is unnecessary to form $Ni_2(L)(CS_2)_2$, as these species are formed in a one-pot reaction between 2 equiv of $Ni(COD)_2$, L, and 2 equiv of CS_2. Spectroscopic, crystallographic, and theoretical data all agree with the lack of thermodynamic difference between *syn* and *anti* conformers in $Ni_2(L)(CS_2)_2$ complexes. Electrochemical studies of $Ni_2(L)(CS_2)_2$ reveal two ligand-based reductions and a CS_2-based oxidation. Chemical reduction results in the oxidation of $[CS_2]^{2-}$ to $[CS_2]^0$ followed by its liberation from

the metal. Reaction of $Ni_2(L)(CS_2)_2$ with the N-heterocyclic carbene NHC forms $Ni_2(NHC)_2(CS_2)_2$. Overall, this research indicates that the iminopyridine ligand is labile at Ni(I) and Ni(II) centers and does not provide necessary stabilization for Ni in the oxidation states required for the overall catalytic cycle (especially for Ni(II)). In addition, the bidentate nature of the iminopyridine enables formation of stable and unreactive η^2 adducts of CS_2, which may preclude its activation. Formation of $Ni_2(NHC)_2(CS_2)_2$ containing nearby positioned carbon disulfides represents a new promising avenue in this project. Its electronic structure and reactivity will be investigated. In addition, we are currently studying the formation and reactivity of the $M_2(L)(CO_2)_2$ and $M_2(L)(oxalate)_2$ complexes (M = Ni, Cu), hoping to shed light on the nature of CO_2 and oxalate binding and transformation in this system.

■ ASSOCIATED CONTENT

Ⓢ Supporting Information

Figures, tables, and CIF files giving NMR spectra, X-ray data, and Cartesian coordinates for all computed structures. This material is available free of charge via the Internet at http://pubs.acs.org.

■ AUTHOR INFORMATION

Notes

The authors declare no competing financial interest.

■ ACKNOWLEDGMENTS

We thank Wayne State University (S.G.) and Grand Valley State University (R.L.L.) for funding, Dr. Lew Hryhorczuk for the experimental assistance, and Prof. H. B. Schlegel for helpful discussions. Computational resources were housed and maintained by the Wayne State Grid. Erwyn Tabasan thanks the Office of Undergraduate Research at Wayne State University for the Undegraduate Research and Creative Projects Award.

■ REFERENCES

(1) Thomas, C. M. *Comments Inorg. Chem.* **2011**, *32*, 14.

(2) For selected recent examples of the cooperative reactivity of dinuclear/multinuclear complexes in binding and activation of small molecules, see: (a) Alliger, G. E.; Müller, P.; Cummins, C. C.; Nocera, D. G. *Inorg. Chem.* **2010**, *49*, 3697. (b) Eames, E. V.; Harris, T. D.; Betley, T. A. *Chem. Sci.* **2012**, *3*, 407. (c) Huang, D.; Holm, R. H. *J. Am. Chem. Soc.* **2010**, *132*, 4693. (d) Lionetti, D.; Day, M. W.; Agapie, T. *Chem. Sci.* **2013**, *4*, 785. (e) Zhao, H. C.; Mello, B.; Fu, B.-L.; Chowdhury, H.; Szalda, D. J.; Tsai, M.-K.; Grills, D. C.; Rochford, J. *Organometallics* **2013**, *32*, 1832.

(3) For selected reviews on CO_2 activation, see: (a) Sakakura, T.; Choi, J.-C.; Yasuda, H. *Chem. Rev.* **2007**, *107*, 2365. (b) Benson, E. E.; Kubiak, C. P.; Sathrum, A. J.; Smieja, J. M. *Chem. Soc. Rev.* **2009**, *38*, 89.

(4) For selected reviews on CS_2 activation, see: (a) Ibers, J. A. *Chem. Soc. Rev.* **1982**, *11*, 57. (b) Pandey, K. K. *Coord. Chem. Rev.* **1995**, *140*, 37.

(5) For selected examples of CO_2 binding and activation, see: (a) Aresta, M.; Nobile, C. F.; Albano, V. G.; Forni, E.; Manassero, M. *J. Chem. Soc., Chem. Commun.* **1975**, 636. (b) Fachinetti, G.; Floriani, C.; Zanazzi, P. F. *J. Am. Chem. Soc.* **1978**, *100*, 7405. (c) Field, J. S.; Haines, R. J.; Sundermeyer, J.; Woollam, S. F. *J. Chem. Soc., Chem. Commun.* **1990**, 985. (d) Wang, T.-F.; Hwu, C.-C.; Tsai, C.-W.; Lin, K.-J. *Organometallics* **1997**, *16*, 3089. (e) Lee, C. H.; Laitar, D. S.; Müller, P.; Sadighi, J. P. *J. Am. Chem. Soc.* **2007**, *129*, 13802. (f) Lu, C. C.; Sauoma, C. T.; Day, M. W.; Peters, J. C. *J. Am. Chem. Soc.* **2007**, *129*, 4. (g) Calabrese, J. C.; Herskovitz, T.; Kinney, J. B. *J. Am. Chem. Soc.* **1983**, *105*, 5914. (h) Angamuthu, R.; Byers, P.; Lutz, M.; Spek, A. L.; Bouwman, E. *Science* **2010**, *327*, 313.

(6) For selected examples of CS_2 binding and activation, see: (a) Poppitz, W. *Z. Anorg. Allg. Chem.* **1982**, *489*, 67. (b) Baird, M.; Hartwell, G., Jr.; Mason, R.; Rae, A. I. M.; Wilkinson, G. *Chem. Commun.* **1967**, 92. (c) Bianchini, C.; Masi, D.; Mealli, C.; Meli, A. *Inorg. Chem.* **1984**, *23*, 2838. (d) Farrar, D. H.; Gukathasan, R. R.; Morris, S. A. *Inorg. Chem.* **1984**, *23*, 3258. (e) Leoni, P.; Pasquali, M.; Fadini, L.; Albinati, A.; Hofmann, P.; Metz, M. *J. Am. Chem. Soc.* **1997**, *119*, 8625. (f) Anderson, J. S.; Iluc, V. M.; Hillhouse, G. L. *Inorg. Chem.* **2010**, *49*, 10203. (g) Haack, P.; Limberg, C.; Tietz, T.; Metzinger, R. *Chem. Commun.* **2011**, *47*, 6374. (h) Livanov, K.; Madhu, V.; Balaraman, E.; Shimon, L. J. W.; Diskin-Posner, Y.; Neumann, R. *Inorg. Chem.* **2011**, *50*, 11273. (i) Maj, J. J.; Rae, A. D.; Dahl, L. F. *J. Am. Chem. Soc.* **1982**, *104*, 4278. (j) Mason, M. G.; Swepston, P. N.; Ibers, J. A. *Inorg. Chem.* **1983**, *22*, 411. (k) Bianchini, C.; Mealli, C.; Meli, A.; Sabat, M. *Inorg. Chem.* **1984**, *23*, 4125. (l) Matson, E. M.; Forrest, W. P.; Fanwick, P. E.; Bart, S. C. *J. Am. Chem. Soc.* **2011**, *133*, 4948. (m) Huang, N.; Li, X.; Xu, W.; Sun, H. *Inorg. Chim. Acta* **2013**, *349*, 446.

(7) Krogman, J. P.; Foxman, B. M.; Thomas, C. M. *J. Am. Chem. Soc.* **2011**, *133*, 14582.

(8) Rail, M. D.; Berben, L. A. *J. Am. Chem. Soc.* **2011**, *133*, 18577.

(9) (a) Hruszkewycz, D. P.; Wu, J.; Green, J. C.; Hazari, N.; Schmeier, T. J. *Organometallics* **2012**, *31*, 470. (b) Hruszkewycz, D. P.; Wu, J.; Hazari, N.; Incarvito, C. D. *J. Am. Chem. Soc.* **2011**, *133*, 328.

(10) (a) Bheemaraju, A.; Lord, R. L.; Müller, P.; Groysman, S. *Organometallics* **2012**, *31*, 2120. (b) Bheemaraju, A.; Beattie, J. W.; Lord, R. L.; Martin, P. D.; Groysman, S. *Chem. Commun.* **2012**, *48*, 9595.

(11) (a) Lu, C. C.; Bill, E.; Weyhermüller, T.; Bothe, E.; Wieghardt, K. *J. Am. Chem. Soc.* **2008**, *130*, 3181. (b) Lu, C. C.; Weyhermueller, T.; Bill, E.; Wieghardt, K. *Inorg. Chem.* **2008**, *48*, 6005. (c) van Gastel, M.; Lu, C. C.; Wieghardt, K.; Lubitz, W. *Inorg. Chem.* **2009**, *48*, 2626. (d) McDaniel, A. M.; Tseng, H.-W.; Hill, E. A.; Damrauer, N. H.; Rappe, A. K.; Shores, M. P. *Inorg. Chem.* **2013**, *52*, 1368. (e) Myers, T. W.; Berben, L. A. *Inorg. Chem.* **2012**, *51*, 1480. (f) Summerscales, O. T.; Myers, T. W.; Berben, L. A. *Organometallics* **2012**, *31*, 3463. (g) Myers, T. W.; Kazem, N.; Stoll, S.; Britt, R. D.; Shanmugam, M.; Berben, L. A. *J. Am. Chem. Soc.* **2011**, *133*, 8662. (h) Nayek, H. P.; Arleth, N.; Trapp, I.; Loeble, M.; Ona-Burgos, P.; Kuzdrowska, M.; Lan, Y.; Powell, A. K.; Breher, F.; Roesky, P. W. *Chem. Eur. J.* **2011**, *17*, 10814. (i) Trifonov, A. A.; Gudilenkov, I. D.; Larionova, J.; Luna, C.; Fukin, G. K.; Cherkasov, A. V.; Poddel'sky, A. I.; Druzhkov, N. O. *Organometallics* **2009**, *28*, 6707.

(12) Aharoni, A.; Vidavsky, Y.; Diesendruck, C. E.; Ben-Asuly, A.; Goldberg, I.; Lemcoff, N. G. *Organometallics* **2011**, *30*, 1607.

(13) (a) Li, C.; Sun, F.-A.; He, M.-Y.; Xu, H.; Chen, Q. *Acta Crystallogr., Sect. E: Struct. Rep.* **2009**, *65*, 286. (b) Chakraborty, B.; Halder, P.; Paine, T. K. *Dalton Trans.* **2011**, *40*, 3647. (c) Zhang, Z.-H.; Chen, S.-C.; He, M.-Y.; Li, C.; Chen, Q.; Du, M. *Cryst. Growth Des.* **2011**, *11*, 5171.

(14) Bianchini, C.; Ghilardi, C. A.; Meli, A.; Midollini, S.; Orlandini, A. *Chem. Commun.* **1983**, 753.